

**FT-IR, RAMAN, NMR, AND DFT, TD-DFT/B3LYP INVESTIGATIONS OF 1-(BENZYLOXY)UREA\*\*****N. Öztürk<sup>1\*</sup>, H. Gökce<sup>2\*</sup>**

<sup>1</sup> Dereli Vocational School, Giresun University,  
28950, Giresun, Turkey; e-mail: nuri.ozturk@giresun.edu.tr

<sup>2</sup> Vocational School of Health Services, Giresun University,  
28200, Giresun, Turkey; e-mail: halil.gokce@giresun.edu.tr

The structural, geometric, spectroscopic, and electronic properties of the 1-(benzyloxy)urea ( $C_8H_{10}N_2O_2$ ) molecule were investigated using experimental and computational methods. The experimental studies were performed via FT-IR, Raman, and NMR spectroscopies for the determination of vibrational and magnetic properties of the title compound. The molecular geometry optimization, vibrational wavenumbers, proton and  $^{13}C$  NMR chemical shifts (in DMSO), HOMO-LUMO analyses, and UV-Vis spectral parameters (in DMSO) for the title molecule were computed with the DFT/B3LYP method at the 6-311++G(2d,2p) basis set. The assignments of harmonic vibrational wavenumbers were computed using the VEDA 4 software program in terms of potential energy distribution (PED). The HOMO-LUMO and UV-Vis analyses were used to determine intramolecular charge transfer and electronic transitions in the title molecule. The experimental values of vibrational frequencies and NMR chemical shifts are in a good harmony with the computed values.

**Keywords:** 1-(benzyloxy)urea, vibrational spectroscopy, NMR chemical shift, DFT/B3LYP computation, HOMO-LUMO and UV-Vis analyses.

**ИССЛЕДОВАНИЕ 1-(БЕНЗИЛОКСИ)МОЧЕВИНЫ МЕТОДАМИ ИК-ФУРЬЕ, КР, ЯМР-СПЕКТРОСКОПИИ И ТЕОРИИ ФУНКЦИОНАЛА ПЛОТНОСТИ****N. Öztürk<sup>1\*</sup>, H. Gökce<sup>2\*</sup>**

УДК 543.42;539.143.43

<sup>1</sup> Профессиональная школа Дерели, Университет Гиресун,  
28950, Гиресун, Турция; e-mail: nuri.ozturk@giresun.edu.tr

<sup>2</sup> Профессиональная медицинская школа, Университет Гиресун,  
28200, Гиресун, Турция; e-mail: halil.gokce@giresun.edu.tr

(Поступила 2 ноября 2017)

Экспериментальными и численными методами исследованы структурные, геометрические, спектроскопические и электронные свойства молекулы 1-(бензилокси)мочевина ( $C_8H_{10}N_2O_2$ ). Экспериментальные исследования выполнены с применением ИК-Фурье, КР и ЯМР-спектроскопии для определения колебательных и магнитных свойств. Оптимальная геометрия молекулы, колебательные частоты, химические сдвиги  $^1H$  и  $^{13}C$  ЯМР (в ДМСО), НОМО-LUMO-анализ и параметры спектров в УФ-видимом диапазонах (в ДМСО) рассчитаны методом DFT/B3LYP в базисном наборе 6-311++G(2d,2p). Гармонические колебательные частоты вычислены с помощью программного обеспечения VEDA 4 в терминах распределения потенциальной энергии. Для определения внутримолекулярного переноса заряда и электронных переходов проведен анализ НОМО-LUMO и спектров УФ-видимого диапазонов. Экспериментальные колебательные частоты и химические сдвиги ЯМР находятся в удовлетворительном согласии с рассчитанными.

**Ключевые слова:** 1-(бензилокси)мочевина, колебательная спектроскопия, химический сдвиг ЯМР, расчет методом DFT/B3LYP, анализ НОМО-LUMO и спектров УФ-видимого диапазона.

\*\* Full text is published in JAS V. 86, No. 1 (<http://springer.com/10812>) and in electronic version of ZhPS V. 86, No. 1 ([http://www.elibrary.ru/title\\_about.asp?id=7318](http://www.elibrary.ru/title_about.asp?id=7318); [sales@elibrary.ru](mailto:sales@elibrary.ru)).

**Introduction.** Hydroxyurea, which displays multidirectional biological activities and is currently used in the treatment of various diseases, was first synthesized in 1969. Although the effect of hydroxyurea in slowing the growth of leukocyte cells was observed in 1928, studies on its antibacterial properties and medical use in cancer treatment began in the 1960s [1–3]. It is currently used by patients with sickle cell anemia to diminish the number of aching crises caused by the illness (hinders creation of sickle-shaped red blood cells), to diminish the need for blood transfusions, chronic myelogenous leukemia, myeloproliferative syndrome, essential thrombocytosis, polycythemia vera, and to treat several cancer types such as squamous cell carcinomas and chronic myelogenous leukemia [4, 5].

The aim of this study is investigating the molecular properties, such as structural, vibrational, NMR chemical shifts, and electronic (HOMO, LUMO, and UV-Vis.) of 1-(benzyloxy)urea using experimental and theoretical methods. A detailed investigation on structural, spectroscopic and electronic properties for the molecule is not available in the literature. The quantum chemical computations have been widely used to determine the structural parameters, vibrational frequencies (IR and Raman), magnetic properties ( $^1\text{H}$  and  $^{13}\text{C}$  NMR chemical shifts and NMR spin-spin couplings), electronic parameters (UV-Vis spectral parameters, HOMO, LUMO, NBO, MEP, etc.), thermodynamic properties (enthalpy, entropy, heat capacity, zero-point energy, Gibbs free energy, Helmholtz free energy, etc.) and nonlinear optical properties of molecular systems, without experimental data. Additionally, the quantum chemical computations provide a powerful support for experimental studies.

**Computational methods.** The geometry optimization, vibrational wavenumbers,  $^1\text{H}$  and  $^{13}\text{C}$  NMR chemical shifts (in DMSO), HOMO-LUMO analyses, and UV-Vis spectroscopic parameters (in DMSO) of the title molecule were computed using the Gaussian 09W program package [6]. A visualization of the calculated results was carried out via the GaussView 5.0 program [7]. In all computations, we used the B3LYP functional (Becke's three parameter exact exchange-functional (B3) combined with the gradient-corrected correlation functional of Lee, Yang, Parr (LYP)) in the density functional theory (DFT) method with the 6-311++G(2d,2p) basis set [8, 9]. The initial geometry for the molecular optimization was taken from ".cif" file generated by single crystal X-ray diffraction of Mai et al. [10, 11]. The vibrational wavenumbers were calculated based on the optimized molecular structure in the gas phase and scaled with 0.9623 [12]. The assignments of the vibrational wavenumbers were performed using VEDA 4 program in terms of potential energy distribution (PED) [13]. Firstly, the optimized molecular geometry of the title molecule was obtained at the B3LYP/6-311++G(2d,2p) level in the DMSO solvent using the conductor-like polarizable continuum model (CPCM) [14] in order to compute the  $^1\text{H}$  and  $^{13}\text{C}$  NMR isotropic chemical shifts and UV-Vis spectral parameters. Then, the  $^1\text{H}$  and  $^{13}\text{C}$  NMR chemical shifts were computed with the mentioned level, model, and solvent using the gauge invariant atomic orbital (GIAO) approach [15–17]. The isotropic absolute shielding values of TMS (tetramethylsilane) with the B3LYP/6-311++G(2d,2p) level were computed as 31.81 ppm for protons and 184.4 ppm for carbons. The  $^1\text{H}$  and  $^{13}\text{C}$  NMR chemical shifts were calculated via the equation  $\delta_{\text{is}}^x = \sigma_{\text{is}}^{\text{TMS}} - \sigma_{\text{is}}^x$  ( $\delta_{\text{is}}^x$  is the isotropic chemical shift and  $\sigma_{\text{is}}^{\text{TMS}}$  and  $\sigma_{\text{is}}^x$  are the isotropic absolute shielding values of TMS and the molecule, respectively). Additionally, the UV-Vis spectral parameters were calculated using the aforementioned computational level, solvent model, and solvent and time dependent DFT (TD-DFT) method [18]. The frontier molecular orbitals (HOMO and LUMO) analyses were performed to determine charge transfers and electronic transitions in the title molecule.

**Results and discussion.** *Molecular structure analysis.* The experimental bond lengths and angles of 1-(benzyloxy)urea were recorded using single crystal X-Ray diffraction by Mai et al. [10, 11]. The space group and unit cell parameters of 1-(benzyloxy)urea are  $P12_1/c1$  (monoclinic) and  $a = 12.456(3)$  Å,  $b = 5.008(1)$  Å,  $c = 13.681(4)$  Å,  $\beta = 96.017(4)^\circ$ ,  $V = 848.7$  Å<sup>3</sup> [10, 11]. The intermolecular hydrogen bonding interactions (N2–H2B $\cdots$ O2<sup>i</sup> and N2–H2A $\cdots$ O2<sup>ii</sup>) in the crystal packing of 1-(benzyloxy)urea were observed between NH<sub>2</sub> and =O groups in the urea group [10, 11]. The computed structural parameters (bond lengths and angles) were obtained with the B3LYP/6-311++G(2d,2p) level in the gas phase. The experimental [10, 11] and computed geometric parameters are listed in Table 1 and compared with each other. The optimized molecular structure is given in Fig. 1. The geometric parameters obtained for 1-(benzyloxy)urea in this study are in good agreement with the structural parameters of similar compounds (1-(3-chlorobenzyl-oxy)urea and 1-(2-fluorobenzyl)-1-(2-fluorobenzyl-oxy)urea) in [19, 20].

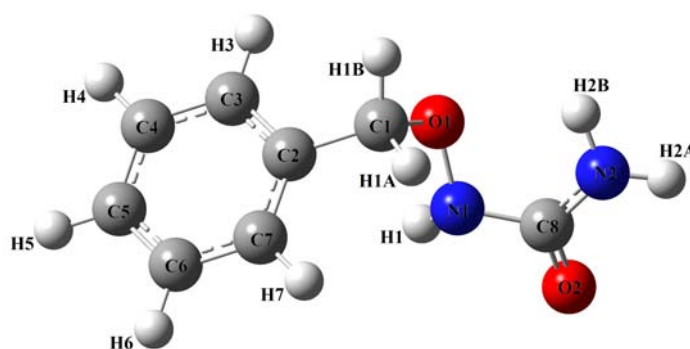


Fig. 1. The optimized molecular structure of 1-(benzyloxy)urea.

The double C=O bond length in the urea group of the compound was experimentally found as 1.220(3) Å, while it was computed as 1.216 Å. The C8–N1 and C8–N2 bond lengths were obtained at 1.274(3)<sub>exp</sub>/1.404<sub>cal</sub> and 1.326(3)<sub>exp</sub>/1.366<sub>cal</sub> Å, respectively. The difference between experimental values of these two C–N lengths (or C8–N2 > C8–N1) resulted from localizations over the N2–H2A and N–H2B bonds in the NH<sub>2</sub> group of electron density and N2–H2B···O2<sup>i</sup> and N2–H2A···O2<sup>ii</sup> intermolecular interactions in the crystal packing [10]. The N1–O1 and C1–O1 bond lengths were obtained as 1.406(2)<sub>exp</sub>/1.418<sub>cal</sub> Å and 1.441(3)<sub>exp</sub>/1.448<sub>cal</sub> Å, respectively. The C1–C2 bond length between phenyl and methylene groups was recorded as 1.392(3) Å and computed as 1.506 Å. The C–C bond lengths in the phenyl ring were measured and calculated at the intervals of 1.279–1.450 and 1.387–1.397 Å, respectively. The C8=O2, C8–N1, C8–N2, N1–O1, C1–O1, and C1–C2 bond lengths were recorded as 1.247(3), 1.387(3), 1.327(3), 1.424(2), 1.439(3), and 1.507(4) Å for 1-(3-chlorobenzyloxy)urea by Mai et al. [19] and measured as 1.229(5), 1.394(5), 1.324(5), 1.424(4), 1.429(6), and 1.499(6) Å for 1-(2-fluorobenzyl)-1-(2-fluorobenzyloxy)urea [20], respectively.

The C2–C1–O1, C1–O1–N1, O1–N1–C8, N1–C8–O2, N1–C8–N2, and O2–C8–N2 bond angles were experimentally measured as 105.3(2)°, 107.5(18)°, 112.7(17)°, 115.2(19)°, 116.4(2)°, and 128.4(19)°, while they were theoretically calculated as 113.1°, 110.0°, 115.1°, 119.7°, 115.2°, and 124.9°, respectively. We can say from some dihedral angle values given in Table 1 that the 1-(benzyloxy)urea molecule is nonplanar. The O1–C1–C2–C3, N1–O1–C1–C2, C1–O1–N1–C8, O1–N1–C8–O2, and O1–N1–C8–N2 dihedral angles were measured at –55.5°, –71.5°, –105.1°, –163.8°, and 19.9° and computed as –72.4°, –71.4°, 129.5°, 159.9°, and 24.6°, respectively.

TABLE 1. Experimental and Calculated Molecular Geometric Parameters of 1-(benzyloxy)urea

Bond lengths (Å)	Experiment [10, 11]	Calc.	Bond angles, degree	Experiment [10, 11]	Calc.	Bond angles, degree	Experiment [10, 11]	Calc.
C1–H1A	0.970	1.090	H1A–C1–H1B	108.8	109.2	C4–C3–H3	120.4	119.9
C1–H1B	0.970	1.090	C2–C1–H1A	110.7	111.2	C6–C5–H5	116.8	120.1
C1–C2	1.392(3)	1.506	O1–C1–H1A	110.7	108.9	C6–C5–C4	126.5(3)	119.8
C1–O1	1.441(3)	1.448	C2–C1–H1B	110.7	111.0	C4–C5–H5	116.8	120.1
C2–C7	1.403(4)	1.395	O1–C1–H1B	110.7	103.1	C3–C4–C5	114.9(3)	120.0
C2–C3	1.450(4)	1.397	C2–C1–O1	105.3(2)	113.1	C3–C4–H4	122.5	119.9
C7–H7	0.930	1.082	C1–C2–C7	117.0	120.9	C5–C4–H4	122.5	120.1
C7–C6	1.282(5)	1.392	C1–C2–C3	118.3(3)	120.2	C1–O1–N1	107.5(18)	110.0
C6–H6	0.930	1.081	C7–C2–C3	124.7(3)	118.9	O1–N1–H1	123.6	110.2
C6–C5	1.417(6)	1.390	C2–C7–H7	122.0	119.5	O1–N1–C8	112.7(17)	115.1
C3–H3	0.930	1.083	C2–C7–C6	115.9(3)	120.6	C8–N1–H1	123.6	111.2
C3–C4	1.279(5)	1.389	C6–C7–H7	122.0	119.9	N1–C8–O2	115.2(19)	119.7
C5–H5	0.930	1.081	C7–C6–H6	120.6	119.9	N1–C8–N2	116.4(2)	115.2
C5–C4	1.407(5)	1.393	C7–C6–C5	118.8(4)	120.0	O2–C8–N2	128.4(19)	124.9
C4–H4	0.930	1.082	C5–C6–H6	120.6	120.1	C8–N2–H2A	120.0	115.1
O1–N1	1.406(2)	1.418	C2–C3–H3	120.4	119.5	C8–N2–H2B	120.0	118.1

Continue Table 1

Bond lengths (Å)	Experiment [10, 11]	Calc.	Bond angles, degree	Experiment [10, 11]	Calc.	Bond angles, degree	Experiment [10, 11]	Calc.
N1–H1	0.860	1.012	C2–C3–C4	119.2(3)	120.6	H2A–N2–H2B	120.0	118.3
N1–C8	1.274(3)	1.404	O1–C1–C2–C3	–55.5	–72.4	C1–O1–N1–H1	74.9	103.7
C8–O2	1.220(3)	1.216	C2–C1–O1–N1	–71.5	–71.4	C2–C3–C4–C5	0.8	0.2
C8–N2	1.326(3)	1.366	O1–N1–C8–O2	–163.8	–159.9	C1–O1–N1–C8	–105.1	–129.5
N2–H2A	0.860	1.005	O1–N1–C8–N2	19.9	24.6	C7–C2–C3–C4	1.8	–0.1
N2–H2B	0.860	1.006						

The reason of the differences between the experimental and computed data is that the theoretical calculations are carried out in the gaseous phase of the isolated molecules, while the experimental records are taken in the solid phase of the compounds. Therefore, the intermolecular interactions in the solid phase of the compounds were ignored in the theoretical computations. Additionally, the anharmonicity negligence, electron correlation effects and basis set deficiencies in the computational methods are the main reasons for the differences between the experimental and theoretical results. The large discrepancies between the structural parameters of 1-(benzyloxy)urea and geometric parameters of similar molecules and the computed molecular geometric parameters may be related to the hydroxyl group etherification and electron delocalization in the urea group [10].

*Vibrational frequencies analysis.* There are 22 atoms and 60 ( $3N-6$ ) vibrational modes of 1-(benzyloxy)urea. The experimental frequencies, computed vibrational parameters (wavenumbers, IR intensities and Raman scattering activities), and their vibrational assignments for the title molecule are listed in Table 2. The vibrational parameters were calculated with the B3LYP/6-311++G(2d,2p) level in the gas phase. The experimental [21] and simulated IR and Raman spectra are given in Fig. 2. The simulated Raman intensity spectra were obtained via the Chemcraft program ([www.chemcraftprog.com](http://www.chemcraftprog.com)).

The  $\text{NH}_2$  group shows stretching bands in the regions of  $3330\text{--}3550\text{ cm}^{-1}$  (asymmetric) and  $3250\text{--}3450\text{ cm}^{-1}$  (symmetric) [22]. The absorption band observed at  $3398\text{ cm}^{-1}$  in the IR spectrum and  $3387\text{ cm}^{-1}$  in the Raman one was assigned to the asymmetric stretching mode of  $\text{NH}_2$ , while the  $\text{NH}_2$  asymmetric stretching vibration was observed at  $3300\text{ cm}^{-1}$  in the IR spectrum [23]. These bands were computed at  $3579$  and  $3460\text{ cm}^{-1}$  with 98% and 96% contributions of PED, respectively. The scissoring mode for  $\text{NH}_2$  was observed at  $1494\text{ cm}^{-1}$  in the IR spectrum, while it was computed at  $1544\text{ cm}^{-1}$  with PED contribution of 82%. The other deformation (rocking, twisting and wagging) modes of  $\text{NH}_2$  were found at ( $\text{cm}^{-1}$ )  $1087$  (IR)– $1102$  (R) $_{\text{exp}}/1078$  $_{\text{cal}}$  for  $\text{pNH}_2$ ,  $562$  (IR)– $560$  (R) $_{\text{exp}}/539$  $_{\text{cal}}$  and  $495$  (IR)– $494$  (R) $_{\text{exp}}/507$  $_{\text{cal}}$  for  $\text{tNH}_2$  and  $445$  (IR)– $444$  (R) $_{\text{exp}}/427$  $_{\text{cal}}$  and  $416$  (IR) $_{\text{exp}}/414$  $_{\text{cal}}$  for  $\text{wNH}_2$ .

The NH stretching band in the urea group was observed at  $3225$  (IR)– $3218$  (R)  $\text{cm}^{-1}$ , while it was calculated at  $3422\text{ cm}^{-1}$  with the PED contribution of 97%. The NH in-plane and out-of-plane bending ( $\delta\text{HNO}$  and  $\tau\text{HNOC}$ ) vibrations were observed at  $1361$  and  $647\text{ cm}^{-1}$  and computed at  $1366$  and  $635\text{ cm}^{-1}$  with 68% and 38% contributions of PED, respectively.

The CH stretching vibrations in the aromatic compounds give rise to the absorption bands in the region of  $3000\text{--}3100\text{ cm}^{-1}$ , whereas the CH bonds with  $sp^3$  hybrid (such as methyl, methylene, etc.) cause stretching bands at the interval of  $2800\text{--}3000\text{ cm}^{-1}$  [22–25]. The aromatic CH stretching vibrations were observed at  $3031\text{--}3089\text{ cm}^{-1}$  in the IR spectrum and  $3007\text{--}3059\text{ cm}^{-1}$  in Raman one. These bands were computed at the interval of  $3046\text{--}3076\text{ cm}^{-1}$ . The stretching vibrations of the methylene group were obtained at  $2954$  (IR)– $2955$  (R) $_{\text{exp}}/2987$  $_{\text{cal}}$   $\text{cm}^{-1}$  for the asymmetric stretching mode and  $2926$  (IR)– $2927$  (R) $_{\text{exp}}/2938$  $_{\text{cal}}$   $\text{cm}^{-1}$  for the symmetric one. The scissoring, wagging, twisting and rocking modes for the methylene group were obtained at  $1419$  (IR)– $1435$  (R) $_{\text{exp}}/1429$  $_{\text{cal}}$   $\text{cm}^{-1}$  for  $\delta_s\text{CH}_2$ ,  $1328$  (IR)– $1327$  (R) $_{\text{exp}}/1329$  $_{\text{cal}}$   $\text{cm}^{-1}$  for  $\text{wCH}_2$ ,  $1211$  (IR)– $1213$  (R) $_{\text{exp}}/1225$  $_{\text{cal}}$   $\text{cm}^{-1}$  for  $\text{tCH}_2$ , and  $971$  $_{\text{cal}}$   $\text{cm}^{-1}$  for  $\text{pCH}_2$ . Additionally, the CH in-plane and out-of-plane bending vibrations in the aromatic ring give rise to the absorption bands in the regions of  $1000\text{--}1600$  and  $650\text{--}1000\text{ cm}^{-1}$ , respectively [22–25]. As expected, the CH in-plane and out-of-plane bending vibrational modes in the phenyl ring of the title molecule were observed and computed in the aforementioned regions.

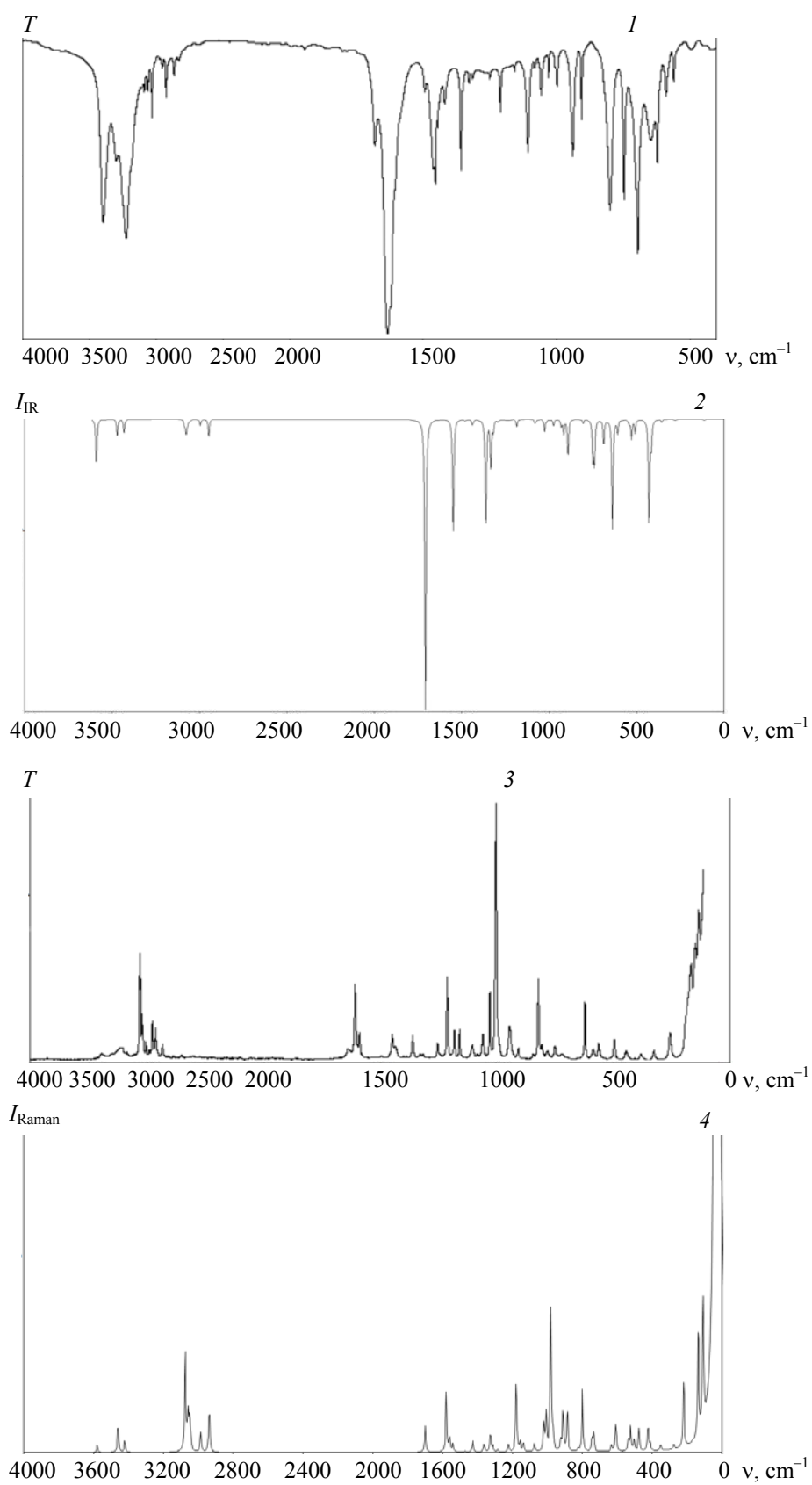


Fig. 2. The experimental (1, 3) and simulated (2, 4) IR (1, 2) and Raman (3, 4) spectra of 1-(benzyloxy)urea.

TABLE 2. Experimental and Calculated Vibrational Wavenumbers ( $\nu$ ,  $\text{cm}^{-1}$ ) of 1-(Benzyloxy)urea and their Assignments

Selected vibrational assignments (PED%)	$\nu_{\text{exp}}$ [21]		B3LYP/6-311++G(2d,2p)		
	IR	Raman	$\nu$	$I_{\text{IR}}$	$S_{\text{Raman}}$
wNH <sub>2</sub> (20) + $\tau$ CCCC(16) + $\delta$ NOC(15)	416	–	414	42.26	0.57
wNH <sub>2</sub> (65)	445	444	427	173.42	2.24
tNH <sub>2</sub> (46) + $\delta$ NCN(11)	495	494	507	21.36	1.27
tNH <sub>2</sub> (35) + $\delta$ OCN(26) + $\delta$ NCN(12)	562	560	539	8.40	1.54
$\delta$ CCC(87) or $\delta$ phenyl(87)	623	621	613	0.44	3.83
$\tau$ HNOC(38) + $\gamma$ ONNC(13) + $\nu$ NO(12)	647	–	635	179.68	1.03
$\nu$ C <sub>1</sub> O <sub>1</sub> (32) + $\tau$ HCCC(27)	–	842	889	60.83	10.73
$\nu$ C <sub>8</sub> N <sub>1,2</sub> (56) + $\nu$ C <sub>1</sub> O <sub>1</sub> (14)	–	–	928	12.43	2.93
$\rho$ CH <sub>2</sub> (36)	–	–	971	9.91	4.21
[ $\delta$ CCC(47) + $\nu$ CC(47)] or $\delta$ phenyl(94)	998	–	984	0.19	41.43
$\nu$ NO(56) + $\nu$ C <sub>1</sub> O <sub>1</sub> (16)	1030	1030	1023	20.62	8.74
$\nu$ CC(37) + $\delta$ HCC(33)	1058	1060	1070	4.03	0.59
$\rho$ NH <sub>2</sub> (59) + $\nu$ C <sub>8</sub> N <sub>2</sub> (10)	1087	1102	1078	6.63	2.80
$\nu$ C <sub>1</sub> C <sub>2</sub> (40) + $\nu$ CC(17) + $\delta$ CCC(12)	–	1181	1181	13.39	27.68
tCH <sub>2</sub> (65)	1211	1213	1225	2.54	3.09
$\nu$ CC(57)	1251	1256	1288	3.13	1.09
wCH <sub>2</sub> (59) + $\delta$ HCC(13)	1328	1327	1329	80.54	9.37
$\nu$ C <sub>8</sub> N <sub>1,2</sub> (50) + $\delta$ HNC(17) + $\delta$ OCN(13) + $\delta$ HNO(12)	1359	–	1358	178.80	0.42
$\delta$ HNO(68)	–	1361	1366	1.29	3.97
$\delta_s$ CH <sub>2</sub> (79)	1419	1435	1429	4.19	5.77
$\delta_s$ NH <sub>2</sub> (82)	1494	–	1544	185.61	5.43
$\nu$ CC(49) + $\delta$ CCC(23)	–	1589	1563	0.47	8.92
$\nu$ CC(53) + $\delta$ HCC(14)	–	1608	1582	0.18	38.84
$\nu$ C=O(74)	1634	1636	1702	478.40	22.92
$\nu_s$ CH <sub>2</sub> (98)	2926	2927	2938	28.50	115.58
$\nu_{\text{as}}$ CH <sub>2</sub> (99)	2954	2955	2987	10.79	57.37
$\nu$ CH(99)	–	3007	3046	3.15	27.73
$\nu$ CH(94)	3031	3043	3051	0.65	82.91
$\nu$ CH(91)	–	3059	3059	8.12	101.26
$\nu$ CH(89)	3064	–	3067	23.15	24.63
$\nu$ CH(99)	3089	–	3076	10.56	314.34
$\nu$ NH(97)	3225	3218	3422	22.72	49.80
$\nu_s$ NH <sub>2</sub> (96)	3300	–	3460	28.75	128.60
$\nu_{\text{as}}$ NH <sub>2</sub> (98)	3398	3387	3579	75.83	39.47

Note.  $\nu$ , stretching;  $\delta$ , in-plane bending;  $\tau$ , torsion;  $\gamma$ , out-of-plane bending;  $\delta_s$ , scissoring;  $\rho$ , rocking; t, twisting; w, wagging;  $I_{\text{IR}}$ , IR intensity (km/mol);  $S_{\text{Raman}}$ , Raman scattering activity; PED, potential energy distribution.

The C=O stretching band in amide groups gives strong absorption bands in the regions of 1670–1620  $\text{cm}^{-1}$  for unsubstituted amides and 1680–1630  $\text{cm}^{-1}$  for N-substituted amides [22]. In this connection, the observed band at 1634 (IR)–1636 (R)  $\text{cm}^{-1}$  was assigned to the C=O stretching vibration. This band was calculated at 1702  $\text{cm}^{-1}$  with 74% contribution of PED. The  $\nu$ C<sub>1</sub>O<sub>1</sub> stretching vibration for the compound was recorded at 842  $\text{cm}^{-1}$  in the Raman spectrum, while it was computed at 889  $\text{cm}^{-1}$  with 32% contribution of PED. The C<sub>8</sub>N<sub>1,2</sub> stretching modes in the urea group of the title molecule were obtained at 1359 (IR) (exp.)/1358 (cal. with 50% contribution of PED)  $\text{cm}^{-1}$  for the asymmetric ( $\nu_{\text{as}}$ N<sub>1</sub>–C<sub>8</sub>–N<sub>2</sub>) stretching vibration and 928 (cal. with 50% contribution of PED)  $\text{cm}^{-1}$  for symmetric ( $\nu_s$ N<sub>1</sub>–C<sub>8</sub>–N<sub>2</sub>) one. The NO stretching vibration was observed at 1030  $\text{cm}^{-1}$  in both IR and Raman spectra, while it was theoretically calculated at 1023  $\text{cm}^{-1}$ .

The aromatic CC stretching vibrations were experimentally recorded at 1608 (R), 1589 (R), 1251 (IR)–1256 (R), and 1058 (IR)–1060 (R)  $\text{cm}^{-1}$ , i.e., in the region of 1600–1000  $\text{cm}^{-1}$  as combined with the CH in-plane bending ( $\delta_{\text{HCC}}$ ) modes of the aromatic ring [23, 26]. Likewise, the in-plane bending deformation modes

( $\delta_{\text{phenyl}}$ ) of the phenyl ring were assigned to 623 (IR)–621 (R) and 998 (IR)  $\text{cm}^{-1}$ , while they were calculated at 613 and 939  $\text{cm}^{-1}$  with the PED contributions of 87% and 94%, respectively. The  $\nu_{\text{C}_1\text{C}_2}$  stretching band between  $\text{C}_1$  atom in the methylene group and  $\text{C}_2$  atom in the phenyl ring was observed at 1181  $\text{cm}^{-1}$  in the Raman spectrum of the title compound. This band was computed at 1181  $\text{cm}^{-1}$  with the PED contribution of 40%.

*NMR chemical shift analysis.* The experimental (in DMSO- $d_6$ ) [21] and calculated (with GIAO method at the B3LYP/6-311++G(2d,2p) level in DMSO using the CPCM solvent model)  $^1\text{H}$  and  $^{13}\text{C}$  NMR isotropic chemical shift values are listed in Table 3.

TABLE 3. Experimental [21] and Calculated  $^1\text{H}$  and  $^{13}\text{C}$  NMR Chemical Shifts of 1-(Benzyloxy)urea (in DMSO- $d_6$ )

Atom	$\delta_{\text{exp}}$	$\delta_{\text{cal}}$	Atom	$\delta_{\text{exp}}$	$\delta_{\text{cal}}$
C1	77.2	84.5	H1	9.07	6.15
C2	136.5	144.9	H1A/H1B	4.73/4.73	4.71/5.12
C3	128.1	137.3	H2A/H2B	6.38/6.38	4.64/5.98
C4	128.6	135.4	H3	7.42	7.94
C5	127.9	135.4	H4	7.37	7.91
C6	128.6	134.4	H5	7.32	7.87
C7	128.1	137.8	H6	7.37	7.82
C8	160.8	169.5	H7	7.42	7.79

Carbonyl carbons such as those in esters, carboxylic acids, amides, ketones, and aldehydes, in which the  $sp^2$  carbon is bonded by a  $\pi$ -bond to the highly electronegative O, give the NMR chemical shift signals in the region of 160–220 ppm [27–29]. The NMR signal for C8 carbon atom in the amide group of the title molecule was observed at 160.8 ppm, while it was computed at 169.5 ppm. The carbons atoms in the methyl and methylene groups bound to an electronegative atom give NMR signals in the region of 55–85 ppm [27–29]. The measured and computed NMR chemical shifts for C2 carbon atom were found at 77.2 and 84.5 ppm, respectively. Aromatic carbons give signals between 120–140 ppm [29]. Phenyl carbons in the title compound were recorded at the interval of 127.9–136.4 ppm, and they were calculated in the region of 134.4–144.9 ppm.

Hydrogen attached to amide nitrogen can be variable in the region of 5–9 ppm of the chemical shift, depending on the effects such as temperature, concentration and solvent [27]. H1, H2A, and H2B protons in the  $\text{NH}_2$  and NH groups caused the NMR signals at 9.07, 6.38, and 6.38 ppm, while they were calculated at 6.15, 4.64, and 5.98 ppm, respectively. The aromatic rings produce large deshielding effects and their  $\pi$ -bonding electrons act as a conductor; the protons attached to carbon atoms in the aromatic rings give resonance signals in the region of 6–8 ppm [27–29]. Aromatic protons in the title molecule were recorded at 7.32–7.42 ppm and computed at 7.79–7.94 ppm.

*HOMO, LUMO, and UV-Vis analyses.* The highest occupied molecular orbital (HOMO) and the lowest unoccupied molecular orbital (LUMO) play an important role in chemical reactions [30]. HOMO and LUMO can be employed to assess donor and acceptor properties of the molecule; also they can be used for the determination of charge transfers to/from the molecule. The molecular properties such as ionization potential and electron affinity can be obtained by considering the HOMO and LUMO energy values. The plots of HOMOs (H and H–1) and LUMOs (L and L+1) and their energy values computed at the B3LYP/6-311++G(2d,2p) level of the title compound are given in Fig. 3. The energy values of the HOMO, LUMO, HOMO–LUMO, and HOMO–1–LUMO+1 band gaps for 1-(benzyloxy)urea were calculated as –7.169, –0.883, 6.286, and 6.626 eV, respectively. One can clearly see from Fig. 4 that two upper filled orbitals are localized on the six-membered aromatic ring and are related to  $\pi$  MO of the  $e_{1g}$  symmetry of the benzene molecule. Similarly, two lower unfilled orbitals have the same localization and are related to  $\pi$  MO of the  $e_{2u}$  symmetry of the benzene molecule.

The computations of UV-Vis spectral properties of the title compound were performed with the TD-DFT/B3LYP/6-311++G(2d,2p) level. The computed UV-Vis electronic absorption wavelengths, oscillator strengths, excitation energies, and major contributions for electronic transitions (obtained by GaussSum 3.0 program [31]) are listed in Table 4. The simulated UV-Vis spectrum of the title molecule is given in Fig. 4. The lowest energy transition has excitation energy of 5.79 eV ( $\lambda = 214$  nm and  $f = 0.09$ ) and is determined by the excitations in the form H→L (73%) and H–1→L+1 (17%). Therefore, it will be localized to the ben-

zene ring, and it is of the type  $\pi \rightarrow \pi^*$ . A high-intensity transition with excitation energy of 6.43 eV ( $\lambda = 193$  nm and  $f = 0.37$ ) is also the transition of the  $\pi \rightarrow \pi^*$  type. It seems that these two electronic transitions are adequate for the characterization of the UV spectra. The contribution of other computed electronic transitions can be considered as sufficiently small.

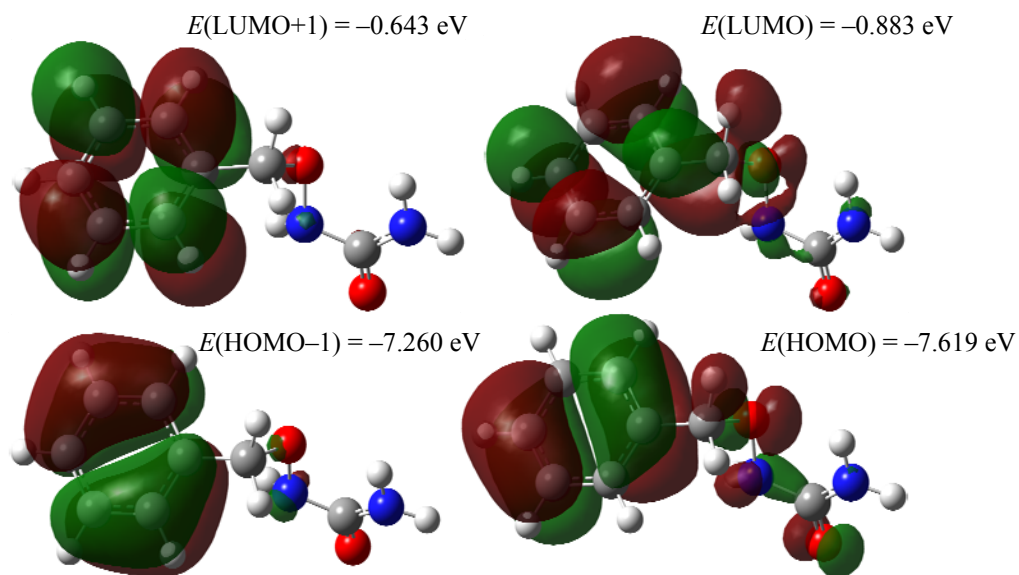


Fig. 3. The simulated HOMOs and LUMOs plots and the energy values of 1-(benzyloxy)urea.

TABLE 4. UV-Vis Parameters Calculated in DMSO of 1-(Benzyloxy)urea

$\lambda$ , nm	Transition	Excitation energy, eV	Oscillator strengths $f$	Major contributions
<b>214</b>	$\pi \rightarrow \pi^*$	<b>5.79</b>	<b>0.09</b>	<b>H<math>\rightarrow</math>L (73%), H-1<math>\rightarrow</math>L+1 (17%)</b>
200	–	6.21	0.04	H-2 $\rightarrow$ L+1 (67%), H $\rightarrow$ L+2 (22%)
198		6.25	0.03	H-3 $\rightarrow$ L (55%), H-4 $\rightarrow$ L (16%), H-1 $\rightarrow$ L+1 (10%)
197		6.29	0.02	H-1 $\rightarrow$ L+2 (80%), H-1 $\rightarrow$ L+3 (12%)
<b>193</b>	$\pi \rightarrow \pi^*$	<b>6.43</b>	<b>0.37</b>	<b>H<math>\rightarrow</math>L+1 (33%), H-1<math>\rightarrow</math>L (24%), H-3<math>\rightarrow</math>L+1 (10%)</b>
192	–	6.47	0.16	H-4 $\rightarrow$ L (42%), H-3 $\rightarrow$ L (31%), H-1 $\rightarrow$ L+1 (12%)
191		6.50	0.04	H-2 $\rightarrow$ L+2 (67%), H $\rightarrow$ L+3 (10%)

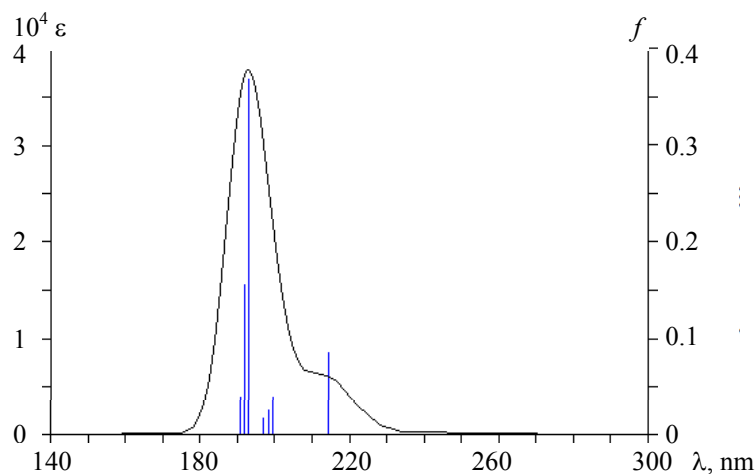


Fig. 4. The simulated UV-Vis spectrum of 1-(benzyloxy)urea.



**Conclusion.** The molecular structure, vibrational wavenumbers (FT-IR and Raman),  $^1\text{H}$  and  $^{13}\text{C}$  NMR isotropic chemical shifts, HOMO and LUMO data, and UV-Vis electronic absorption parameters for 1-(benxyloxy)urea were investigated using experimental and computational methods. The experimental structural and spectroscopic properties (vibrational wavenumbers and NMR chemical shifts) were supported by the data computed with the DFT/B3LYP/6-311++G(2d,2p) level. The electronic transitions corresponding to the theoretical UV-Vis spectral wavelengths were confirmed by HOMO and LUMO analyses of 1-(benxyloxy)urea.

## REFERENCES

1. P. Navarra, P. Preziosi, *Crit. Rev. Oncol./Hematol.*, **29**, 249–255 (1999).
2. N. Saban, M. Bujak, *Cancer Chemother. Pharmacol.*, **64**, 213–221 (2009).
3. R. Hilf, C. Bell, I. Michel, J. J. Freeman, A. Borman, *Cancer Res.*, **26**, 2286–2291 (1966).
4. B. Chabner, P. Calabresi, *Chemotherapy of Neoplastic Disease*, The Pharmacological Basis of Therapeutics, 10<sup>th</sup> ed., McGraw-Hill, New York, 1388–1445 (2001).
5. S. Hardjono, S. Siswodihardjo, P. Pramono, W. Darmanto, *Chem. Chem. Technol.*, **11**, No. 1, 19–24 (2017).
6. *Gaussian 09, Revision D.01*, Gaussian Inc., Wallingford CT (2009).
7. R. Dennington, T. Keith, J. Millam, *GaussView*, Version 5, Semichem Inc., Shawnee Mission KS (2009).
8. A. D. Becke, *J. Chem. Phys.* **98**, 5648–5652 (1993).
9. C. Lee, W. Yang, R. G. Parr, *Phys. Rev. B*, **37**, 785–789 (1988).
10. X. Mai, H.-Y. Xia, Y.-S. Cao, X.-S. Lu, Y.-J. Liao, *Z. Kristallogr. NCS*, **224**, 547–548 (2009).
11. X. Mai, X. Lu, H. Xia, Y. Cao, Y. Liao, X. Lv, *Chem. Pharm. Bull.*, **58**, No. 1, 94–97 (2010).
12. J. M. Alia, H. G. M. Edwards, *J. Phys. Chem. A*, **109**, 7977–7987 (2005).
13. M. H. Jamroz, *Vibrational Energy Distribution Analysis VEDA4* (Warsaw, 2004).
14. S. Miertus, E. Scrocco, J. Tomasi, *J. Chem. Phys.*, **55**, 117–129 (1981).
15. F. London, *J. Phys. Radium*, **8**, 397–409 (1937).
16. R. Ditchfield, *Mol. Phys.*, **27**, 789–807 (1974).
17. K. Wolinski, J. F. Himton, P. Pulay, *J. Am. Chem. Soc.*, **112**, 8251–8260 (1990).
18. E. Runge, E. K. U. Gross, *Phys. Rev. Lett.*, **52**, 997–1000 (1984).
19. X. Mai, H.-Y. Xia, Y.-S. Cao, W. Tong, G.-G. Tu, *Acta Crystallogr.*, **E65**, o2983 (2009).
20. X. Mai, H.-Y. Xia, Y.-S. Cao, X.-S. Lu, X.-N. Fang, *Acta Crystallogr.*, **E65**, o442 (2009).
21. National Institute of Advanced Industrial Science and Technology (AIST), Spectral Database for Organic Compounds, SDBS; <http://sdb.sdb.aist.go.jp> Cited September 30, 2017.
22. N. B. Colthup, L. H. Daly, E. Wiberley, *Introduction to Infrared and Raman Spectroscopy*, Academic Press, New York (1964).
23. H. Gökce, S. Bahçeli, *Spectrochim. Acta, Pt A*, **133**, 741–751 (2014).
24. L. J. Bellamy, *The Infrared Spectra of Complex Molecules*, 3<sup>rd</sup> ed., Wiley, New York (1975).
25. R. M. Silverstein, F. X. Webster, *Spectroscopic Identification of Organic Compound*, 6<sup>nd</sup> ed., John Wiley & Sons, New York (1998).
26. H. Buyukuslu, M. Akdogan, G. Yildirim, C. Parlak, *Spectrochim. Acta, A*, **75**, 1362–1369 (2010).
27. D. L. Pavia, G. M. Lampman, G. S. Kriz, J. R. Vyvyan, *Introduction to Spectroscopy*, Brooks/Cole Cengage Learning (2009).
28. J. B. Lambert, H. F. Shurvell, R. G. Cooks, *Introduction to Organic Spectroscopy*, Macmillan, New York (1987).
29. R. J. Anderson, D. J. Bendell, P. W. Groundwater, *Organic Spectroscopic Analysis*, The Royal Society of Chemistry (RSC) Sunderland (2004).
30. K. Fukui, *Science*, **218**, 747–754 (1982).
31. N. M. O'Boyle, A. L. Tenderholt, K. M. Langner, *J. Comput. Chem.*, **29**, 839–845 (2008).